Voltage-dependent Regulation of Modal Gating in the Rat SkM1 Sodium Channel Expressed in *Xenopus* Oocytes

SEN JI,* WEIJING SUN,* ALFRED L. GEORGE, JR,‡ RICHARD HORN,§ and ROBERT L. BARCHI*

From the *Mahoney Institute of Neurological Sciences and the Department of Neuroscience, University of Pennsylvania School of Medicine, Philadelphia, Pennsylvania 19104; ‡Department of Medicine, Vanderbilt University School of Medicine, Nashville, Tennessee 37232; and §Department of Physiology, Thomas Jefferson University School of Medicine, Philadelphia, Pennsylvania 19107

ABSTRACT The TTX-sensitive rat skeletal muscle sodium channel (rSkM1) exhibits two modes of inactivation (fast vs slow) when the α subunit is expressed alone in *Xenopus* oocytes. In this study, two components are found in the voltage dependence of normalized current inactivation, one having a $V_{1/2}$ in the expected voltage range (~ -50 mV, I_N) and the other with a more hyperpolarized $V_{1/2}$ (~ -130 mV, I_H) at a holding potential of -90 mV. The I_N component is associated with the gating mode having rapid inactivation and recovery from inactivation of the macroscopic current (N-mode), while I_H corresponds to the slow inactivation and recovery mode (H-mode). These two components are interconvertible and their relative contribution to the total current varies with the holding potential: I_N is favored by hyperpolarization. The interconversion between the two modes is voltage dependent and is well fit to a first-order two–state model with a voltage dependence of *e*-fold/8.6 mV and a $V_{1/2}$ of -62 mV. When the rat sodium channel β_1-subunit is coinjected with rSkM1, I_H is essentially eliminated and the inactivation kinetics of macroscopic current becomes rapid. These two current components and their associated gating modes may represent two conformations of the α subunit, one of which can be stabilized either by hyperpolarization or by binding of the β_1 subunit.

INTRODUCTION

The voltage-gated sodium channel undergoes a series of voltage- and time-dependent conformational transitions as the channel opens and then inactivates in response to depolarization (for review, see Patlak, 1991). It is commonly assumed that sodium channels in a membrane move through these states by a common path that is characterized by rapid activation and inactivation at the macroscopic current level (Hodgkin and Huxley, 1952), and by clustering of brief openings at the beginning of a depolarizing pulse at the single-channel level (Aldrich, Corey, and

Address correspondence to R. L. Barchi, Institute of Neurological Sciences, 218 Stemmler Hall, University of Pennsylvania School of Medicine, Philadelphia, PA 19104.

J. GEN. PHYSIOL. © The Rockefeller University Press · 0022-1295/94/10/0625/19 $2.00
Volume 104 October 1994 625–643

Stevens, 1983; Horn and Vandenberg, 1984; Sigworth and Neher, 1980). However, such homogeneous gating is not always the case. In addition to the fast gating mode described by the classical Hodgkin-Huxley model, channels can show a slow inactivation mode that is characterized by bursts of openings with prolonged open time. The existence of these modes has been observed in cardiac muscle (Kirsch and Brown, 1989; Kiyosue and Arita, 1988; Nilius, 1988; Patlak and Ortiz, 1985), neuroblastoma cells (Quandt, 1987), Schwann cells (Howe and Ritchie, 1992), and in skeletal muscle (Patlak and Ortiz, 1986) where the slow-gated channels typically comprised ~0.1% of the peak whole-cell current.

The coexistence of these two gating modes is particularly evident when the adult rat skeletal muscle (rSkM1) or brain (IIA or III) sodium channel α subunits are expressed in *Xenopus laevis* oocytes. Several groups have reported the existence of multiple gating modes in the same membrane patch as well as the slow switching between different gating modes in a single channel, corresponding to the presence of two components in the inactivation of the whole-cell current (Auld, Goldin, Krafte, Marshall, Dunn, Catterall, Lester, Davidson, and Dunn, 1988; Krafte, Goldin, Auld, Dunn, Davidson, and Lester 1990; Moorman, Kirsch, VanDongen, Joho, and Brown 1990; Zhou, Potts, Trimmer, Agnew, and Sigworth, 1991). For these channels expressed in oocytes, nearly 50% may be in the slow-gated mode at a given holding potential (Zhou et al., 1991).

While this phenomenon of modal gating has been well described, important questions regarding the regulation and interconversion of different modes and the molecular mechanisms that underlie them remain unanswered. For example, do channels in different modes show altered voltage dependence in their inactivation and their recovery from inactivation? Does membrane potential affect gating mode conversion? Are modes associated with distinct protein conformations?

Our results show that the rSkM1 sodium channel expressed in oocytes can exhibit at least two gating modes that have different voltage dependence of inactivation and of recovery from inactivation, and that the interconversion of channels between these gating modes is a voltage dependent and slow process. Furthermore, the slow gating mode is greatly reduced by coinjection of cRNA encoding a rat sodium channel β_1 subunit with rSkM1. The two modes may be a consequence of alternate tertiary structures assumed by rat SkM1 when expressed in oocytes in the absence of a β_1 subunit, implicating the binding of β_1 as a factor in stabilizing the physiologically preferred channel conformation.

MATERIALS AND METHODS

Preparation of Recombinant RNAs

The full-length cDNA of rSkM1 (Trimmer, Cooperman, Tomiko, Zhou, Crean, Boyle, Kallen, Sheng, Barchi, Sigworth, Goodman, Agnew, and Mandel, 1989) was cloned into pRC/CMV vector (InvitroGen, San Diego, CA). cRNA was generated from the *Not*I linearized plasmid using T7 RNA polymerase and capped with $m^7G(5')ppp(5')G$. After removing template DNA with RNase-free DNase I, cRNA was extracted, precipitated, and stored at −70°C for injection in oocytes.

Preparation of β_1 subunit recombinant RNA was carried out as described previously (Bennett, Makita, and George, 1993). In short, cDNA encoding the β_1 subunit, obtained by

PCR amplification from rat heart, was transferred into pBluescript (Stratagene Corp., La Jolla, CA), and cRNA was transcribed from *EcoR*I linearized pRHβ-M6 using T7 RNA polymerase.

Injection of cRNAs

Xenopus oocytes were isolated enzymatically by treating frog ovarian tissue with 2 mg/ml collagenase solution (Goldin, 1992). Stage III and IV oocytes, which have relatively smaller size and give a faster setting of capacitative current, were selected for RNA injection (Krafte and Lester, 1992). 50 nl cRNA (1 μg/ml) was injected into each oocyte. Injected oocytes were incubated in 50% L-15 solution (Gibco Laboratories, Grand Island, NY) enriched with 10 mM HEPES and 1 mM glutamine and supplemented with 100 U/ml penicillin and 100 μg/ml streptomycin (pH 7.6), at 19°C. Sodium channel expression was detectable 24 h after injection, and was stable for the following 72 h.

Electrophysiological Recording

The two-electrode oocyte clamp technique was used to record expressed sodium currents (Chahine, Chen, Barchi, Kallen, and Horn, 1992; Stühmer, 1992). The oocyte clamp amplifier (OC-725A, Warner Instrument Corp., Hamden, CT) was interfaced with a PC type microcomputer through a TL-1 DMA Interface (Axon Instruments, Inc., Foster City, CA). The pCLAMP software package was used for voltage protocol programming and data acquisition. For those voltage protocols having a conditioning pulse, a very brief pulse (0.5–0.75 ms) to the holding potential was applied between the conditioning and test pulses to reset the channel activation gate. Recording electrodes were fabricated from borosilicate pipette glass (A-M Systems Inc., Seattle, WA) and filled with 3 M KCl. The current electrode, shielded with aluminum foil, had a resistance of ~0.5 MΩ and the voltage electrode had a resistance of 1.0–1.5 MΩ. Capacitative and linear leak currents were subtracted using recordings after blocking sodium current by 10^{-8} M tetrodotoxin. Oocytes were continuously perfused with normal Ringer's solution containing (in millimolar): 115 NaCl, 2.5 KCl, 1.8 $CaCl_2$, 2.0 $MgCl_2$ and 5.0 HEPES (pH 7.5).

Data Analysis

All data points in both figures and text are expressed as mean ± SEM. Curve fitting was carried out using the SigmaPlot Scientific Graph System (Jandel Scientific, Corte Madera, CA). Inactivation curves were fitted to Boltzmann relations shown below:

$$I/I_{max} = 1/\{1 + \exp [ze(V - V_{1/2})/kT]\} \quad (1)$$

or

$$I/I_{max} = (1 - a)/\{1 + \exp [z_N e(V - V_{N,1/2})/kT]\} + a/\{1 + \exp [z_H e(V - V_{H,1/2})/kT)]\} \quad (2)$$

in which z is the apparent inactivation gate valence, $V_{1/2}$ is the membrane potential at which 50% inactivation occurs, e is the elementary charge, k is the Boltzmann constant, T is the absolute temperature, a and $(1 - a)$ are the relative weights of I_H and I_N. Time constants for the recovery of current from inactivation were obtained by fitting data points to the following equations:

$$I(t) = 1 - \exp (-t/\tau) \quad (3)$$

or:

$$I(t) = (1 - a)[1 - \exp (-t/\tau_{slow})] + a[1 - \exp (-t/\tau_{fast})] \quad (4)$$

where τ is the time constant for current to recover from inactivation. Current activation curves

were fit to the following Boltzmann equation:

$$g_{Na}/g_{Na,max} = 1/\{1 + \exp [ze(V_{1/2} - V)/kT]\} \quad (5)$$

in which g_{Na} was calculated by dividing peak Na current by the driving force ($V_m - E_{Na}$), where E_{Na} was estimated by extrapolating the *I-V* curve to zero current level. Current inactivation time constants (τ) and relative amplitude (A) of each component was obtained by fitting the inactivation phase of the current traces, starting at the peak of current, to the following equation:

$$I_{total}(t) = A_{fast} * \exp(-t/\tau_{fast}) + A_{slow} * \exp(-t/\tau_{slow}) + A_{\infty}. \quad (6)$$

Two-state First-order Reaction Model

Distribution of sodium channels between two gating modes (H and N modes, see Results) was fit to a simplified voltage-dependent two-state first-order reaction model, based on the following facts and assumptions: (*a*) the interconversion is voltage dependent (Fig. 2 *A*), but reaches a steady state very slowly (Fig. 2 *B*; Zhou et al., 1991); (*b*) interconversion between modes is different from the rapid gating transitions between various states and mainly occurs at the holding potential; conversion during the test pulse is negligible (Fig. 5); (*c*) normal gating transitions can be combined into a single mode, because gating transitions in a given mode are much faster than modal interconversion (Figs. 2 *B* and 3 *B*). Therefore, the relative weights of the N-mode (W_N) and the H-mode (W_H, or $1 - W_N$) can expressed by the following model:

$$\text{H-mode} \underset{\beta}{\overset{\alpha}{\rightleftharpoons}} \text{N-mode},$$

or

$$1 - W_N \underset{\beta}{\overset{\alpha}{\rightleftharpoons}} W_N.$$

The relative weight of the N-mode is consequently expressed by:

$$dW_N/dt = \alpha(1 - W_N) - \beta W_N. \quad (7)$$

The analytic solution of Eq. 7, which satisfies the initial condition $W_N = W_{N,0}$ when the holding potential is infinitely short ($t = 0$), and the boundary condition $W_N = W_{N,\infty}$ when the distribution between two modes is at equilibrium as t approaches ∞, is

$$W_N = W_{N,\infty} - (W_{N,\infty} - W_{N,0}) * \exp(-t/\tau_N) \quad (8)$$

where

$$\tau_N = 1/(\alpha + \beta) \quad (9)$$

$$W_{N,\infty} = \alpha/(\alpha + \beta). \quad (10)$$

RESULTS

Two Components in Sodium Current Inactivation

A double-pulse protocol was used to assess the availability of sodium channels at different prepulse membrane potentials (Fig. 1 *C*, *inset*). As shown in Fig. 1 *A*, the relationship between normalized peak sodium current and prepulse potential for

rSkM1 expressed in *Xenopus* oocytes does not have a single component. Instead, two components are evident. A large decrease in current amplitude occurs as the potential of the conditioning pulse changes from −180 to −130 mV. After a plateau between −120 and −90 mV, a second decline is seen from −80 to −30 mV. Fitting the ratios of I/I_{max} to a modified Boltzmann relation (Eq. 2, Materials and Methods) yields a normalized inactivation curve having two components, each with a characteristic $V_{1/2}$, apparent gating valence z, and relative weight (Fig. 1 *C* and Table I). We will refer to the component with the more negative $V_{1/2}$ (−125 to −135 mV) as

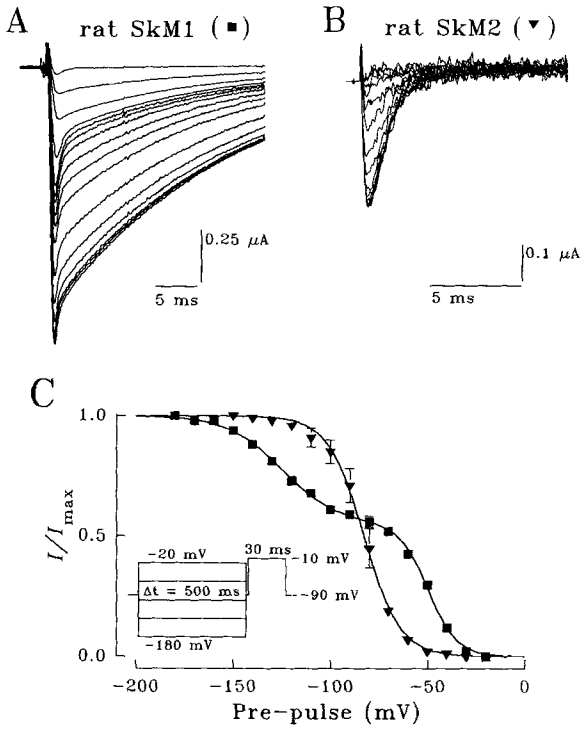

FIGURE 1. Inactivation of the rat SkM1 and SkM2 sodium currents expressed in *Xenopus* oocytes. (*A*) Current traces recorded using a double-pulse protocol (*C, inset*) when rat SkM1 was expressed in oocytes. The double pulse was delivered in an interval of 6 s from a holding potential of −90 mV. (*B*) Current traces recorded using the same voltage protocol when rat SkM2 was expressed. (*C*) Normalized current inactivation curves [SkM1 (■, n = 5) vs SkM2 (▼, n = 3)]. Continuous lines are the best fits to Boltzmann equations (Eqs. 1 and 2). Data points are shown as mean ± SEM. For some points, SEM's are smaller than the size of the symbols. The curve for SkM1 is biphasic, with one component inactivating in the normal voltage range (I_N; $V_{1/2}$ = −49.6 mV, apparent inactivation valence [z_N] = 3.3 elementary charges [e_0], and relative weight [W_N] = 0.55) while the second inactivates at hyperpolarized potentials (I_H, $V_{1/2,H}$ = −124.7 mV, z_H = 1.7 e_0, and W_H = 0.45). For SkM2, $V_{1/2}$ = −82.5 mV, and z = 2.6 e_0.

hyperpolarized current component, or I_H, and that with a $V_{1/2}$ in the normal voltage range of −45 to −55 mV as normal current component, or I_N. The gating mode that produces I_H will be referred to as the H-mode; the mode contributing to I_N as the N-mode.

Such a biphasic inactivation curve was not observed when the same voltage protocol was used to examine sodium currents produced by the tetrodotoxin (TTX)-resistant form of the rat skeletal muscle sodium channel (rSkM2) (Kallen,

Sheng, Yang, Chen, Rogart, and Barchi, 1990) expressed in oocytes under identical conditions (Fig. 1, *B* and *C*).

One possibility that may account for the biphasic shape of the inactivation curve is that the rSkM1 sodium channel protein, encoded by a single mRNA, can assume either of two interconvertible gating modes. If these modes differ in their voltage- and time-dependent gating transitions, then the relative weights of the two components in the inactivation curve should vary as the potential and the duration of the holding pulse is changed. To test this possibility, we first altered the amplitude of the holding potential between double pulses (Fig. 2 *A*). We found that the relative

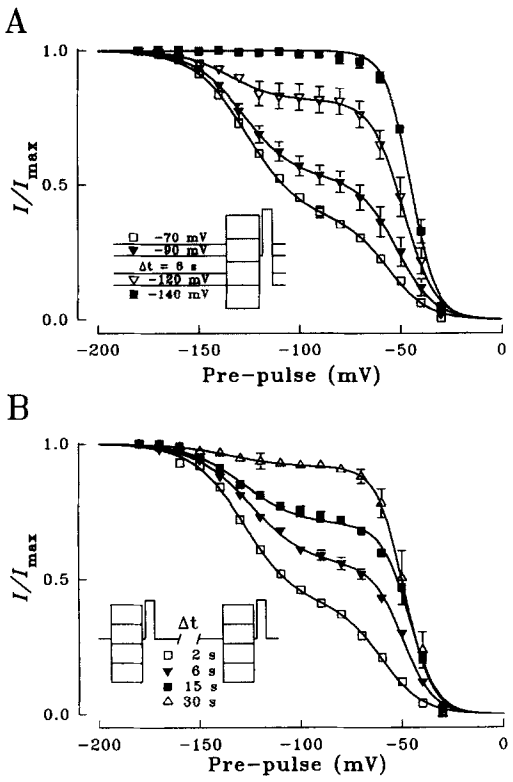

FIGURE 2. Effects of the holding conditions between double pulses on the inactivation of the rat SkM1 sodium current. Voltage protocols are shown by the insets inside the figure. (*A*) Effects of the voltage of the holding pulse (−70 [□], −90 [▼], −120 [▽], and −140 [■] mV). (*B*) Effects of the length of the holding pulse (2 [□], 6 [▼], 15 [■], and 30 [△] s). The relative weights, apparent valences z and $V_{1/2}$'s were altered as the voltage and the duration of the holding pulse were changed (see Table I). Data points are shown as mean ± SEM. Solid lines are the best fits to a modified Boltzmann relationship (Eq. 2).

contribution of the two components shifted dramatically as the holding potential was changed (Fig. 2 *A* and Table I). The contribution of the H-component became significantly smaller as the holding potential changed from −70 to −120 mV and essentially disappeared with a holding potential of −140 mV, indicating a voltage-dependent shift of more channels into the N-mode. Similarly, increasing the duration of the holding pulse between trials also reduced the relative weight of I_H. Conversely, this component became larger when the holding pulse was shortened (Fig. 2 *B* and Table I), suggesting a slow transition between the two components. The relative

weight (W), apparent valence (z), and $V_{1/2}$ of each component for different holding conditions are summarized in Table I.

The relative weights of the two components depend critically on the voltage protocols used. With sufficiently long durations at sufficiently hyperpolarized holding potentials, I_H becomes very small. Thus, the data in Figs. 1 *C* and 2 are not true steady state inactivation curves (or h_∞ curve) under typical conditions (i.e., −90 mV holding potential and 6-s repetition interval). This is due to the very slow rates of recovery from inactivation for channels in the H-mode and interconversion of channels between modes, as we demonstrate below (Fig. 4 *B*).

TABLE I

Effects of the Holding Condition between Double Pulses on rSkM1 Sodium Current Inactivation

	z (Elementary charge)		$V_{1/2}$ (millivolts)		Weight	
	I_H	I_N	I_H	I_N	I_H	I_N
Different holding potentials with the same interval (6 s; n = 7):						
−70 mV	1.8 ± 0.1	2.6 ± 0.1	−124.5 ± 1.5	−54.5 ± 2.0	65 ± 2%	35 ± 2%
−90 mV	1.8 ± 0.1	3.1 ± 0.2	−126.8 ± 2.0	−52.5 ± 3.1	48 ± 3%	52 ± 3%
−120 mV	2.4 ± 0.6	3.5 ± 0.2	−137.4 ± 4.1	−48.0 ± 2.3	16 ± 2%	84 ± 2%
−140 mV	N/A	4.1 ± 0.4	N/A	−44.8 ± 0.8	N/A	100%
Different intervals at the same holding potential (−90 mV; n = 5):						
2 s	1.9 ± 0.1	2.4 ± 0.1	−128.4 ± 0.8	−60.8 ± 1.2	58 ± 2%	42 ± 2%
6 s	1.7 ± 0.1	3.3 ± 0.3	−129.2 ± 2.4	−48.7 ± 0.3	44 ± 3%	56 ± 3%
15 s	1.6 ± 0.1	3.6 ± 0.1	−126.4 ± 2.4	−45.9 ± 0.6	30 ± 2%	70 ± 2%
30 s	1.8 ± 0.2	4.2 ± 0.3	−134.9 ± 4.8	−50.4 ± 1.3	9 ± 2%	91 ± 2%

Voltage Dependence of the Interconversion between Modes

Our data (Fig. 2) suggest that the interconversion between H- and N-modes is a voltage-dependent process and occurs slowly. To understand how voltage controls this interconversion, we assumed a simple first-order two-state model

$$\text{H-mode} \underset{\beta}{\overset{\alpha}{\rightleftharpoons}} \text{N-mode}$$

in which the two modes are linked by single voltage-dependent forward (α) and backward (β) first-order rate constants. We estimated the steady state distribution between the two modes from inactivation experiments using a quadruple-pulse protocol (V_1, V_2, V_3, and V_4) as shown in Fig. 3 *A*. The design of the voltage protocol is detailed in the legend of Fig. 3. The peak current recorded at V_4 was normalized to the maximal peak current and I/I_{max} was then fit to Eq. 2 to obtain the relative weights of the two components (I_N and I_H). Fig. 3 *B* shows the fractional weight of the N-component (W_N) plotted against the duration of holding potential (V_2) for three different voltages (−50, −70, and −90 mV). The theoretical curves are the best fits to

Eq. 8, shown as exponential relaxations. Fig. 3 *C* shows that α and β can be reasonably described as exponential functions of membrane holding potentials: α increases as the membrane is hyperpolarized, and β increases as the membrane is depolarized. Channels are evenly distributed between the two modes at a holding potential of −62 mV, a value that differs from $V_{1/2}$'s of either steady state sodium current activation (~ −20 mV) or inactivation (~ −50 mV). The interconversion has a voltage dependence of *e*-fold change over 8.6 mV, relatively weak as compared with

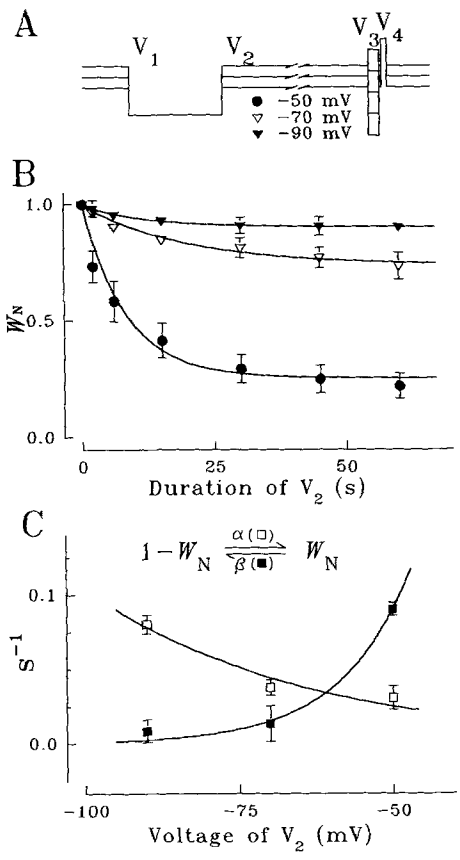

FIGURE 3. Voltage dependence of mode interconversion. (*A*) Voltage protocol used to assess the availability of rSkM1 sodium channels in different modes. The first pulse, V_1 (−140 mV with a duration of 2.5 or 3 s), drives all the channels into the N-mode to assure the same initial condition for interconversion to occur; during the holding potential, V_2 (−50, −70, and −90 mV with various durations of 2, 6, 15, 30, 45, and 60 s), channels convert between the modes; V_3 serves as the conditioning pulse; V_4 tests the availability of channels in different modes. (*B*) Relative weight of the N-component (W_N) as a function of holding potential durations for three different voltages (−50 [●], −70 [▽], and −90 [▼] mV). W_N was obtained by fitting I/I_{max} to Eq. 2. Solid lines are the best fits to Eq. 8. From this analysis, we obtained τ_N,$W_{N,\infty}$ and $W_{N,0}$ for different holding potentials as follows: at −50 mV: 8.3 s, 0.26, 1; at −70 mV: 19.5 s, 0.74, 1; at −90 mV: 11.3 s, 0.9, 1. (*C*) Rate constant (α, forward and β, backward) of the first-order reaction interconverting the N- and H-modes. α (□) and β (■) were calculated from Eqs. 9 and 10. Data points were fit to an exponential dependence on membrane potential. The solid curves are: α = 0.0061 * exp(−0.7112 * *Ve/kT*) and β = 7.2839 * (exp(2.1964 * *Ve/kT*), where *V* is the holding potential, and *e*, *k*, and *T* are defined in the Materials and Methods.

the voltage dependence of sodium channel steady state activation (*e*-fold/4 mV) and inactivation (*e*-fold/6.7 mV) in the normal gating mode (Hodgkin and Huxley, 1952). The interconversion time constants are 8.3, 19.5, and 11.3 s at holding potentials of −50, −70, and −90 mV, respectively, very slow as compared with sodium current activation and inactivation process (Hodgkin and Huxley, 1952).

Two Components in Current Recovery from Inactivation

We then examined the recovery of current from inactivation using a triple-pulse protocol (Fig. 4 *A*, *inset*). Inactivation was induced by a 30-ms depolarization to 20 mV and recovery was measured as the peak current at a test pulse of −10 mV after an interpulse of variable voltages lasting either 50 or 500 ms. The length of the holding pulse (−90 mV) between triple pulses was 30 s. As expected, current recovery from inactivation was biphasic; one component recovered at hyperpolarized potentials and the other recovered at relatively depolarized potentials (Fig. 4 *A*). Furthermore, the normalized recovery curves became flatter, as compared with Fig. 1 *C*, indicating that neither the 50- nor the 500-ms interpulse was long enough to allow channels to recover completely from inactivation at any voltage. A summary of relative weight, gating valence and $V_{1/2}$ is provided in Table II.

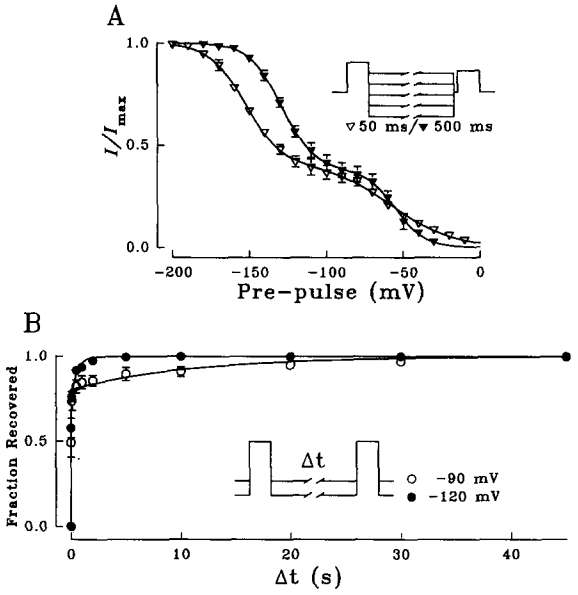

FIGURE 4. Recovery of rat SkM1 sodium current from inactivation. (*A*) Voltage-dependent recovery from inactivation (n = 5). Inactivation was induced by a large depolarization (20 mV). Recovery was assessed by recording current at −10 mV after conditioning pulses of either 50 (▽) or 500 ms (▼) to different potentials. Continuous lines are the best fits to Eq. 2. A summary of $V_{1/2}$'s, gating valences and relative weights is shown in Table II. (*B*) Time course of current recovery from inactivation (n = 3). A double-pulse protocol was used (*B*, *inset*). Two holding potentials (−90 mV [○] and −120 mV [●]) were used and the test voltage was −10 mV. The solid lines are the best fits to Eq. 4. At V_{hold} = −90 mV, τ_{fast} = 2.6 ms and τ_{slow} = 10.8 s; at V_{hold} = −120 mV, τ_{fast} = 1.5 ms and τ_{slow} = 512 ms.

The effects of the interpulse duration on recovery from inactivation was also examined over a wide range at two different holding potentials (−90 vs −120 mV), and the results are plotted in Fig. 4 *B*. The data were well fit by a weighted sum of two exponentials with different time constants (Eq. 4). At a holding potential of −90 mV, two components are especially prominent, one with a time constant of 2.6 ms and the other with a much slower time constant of 10.8 s. At this holding potential, more than 30 s were required for the current to fully recover. At a holding potential of −120 mV, the rate of recovery from inactivation was significantly faster. This was especially true for the recovery of the slow component (τ_{slow} = 512 ms at V_{hold} = −120 mV, but τ_{slow} = 10.8 s at V_{hold} = −90 mV).

TABLE II

Effects of the Condition of the Interpulse on rSkM1 Sodium Current Recovery from Inactivation (n = 4)

	z (elementary charge)		$V_{1/2}$ (millivolts)		Weight	
	I_H	I_N	I_H	I_N	I_H	I_N
50 ms	2.1 ± 0.1	1.4 ± 0.1	−152.8 ± 2.1	−54.3 ± 2.6	60 ± 3%	40 ± 3%
500 ms	2.3 ± 0.2	2.5 ± 0.1	−129.2 ± 1.8	−54.4 ± 1.7	62 ± 4%	38 ± 4%

Amplitude and Inactivation of Macroscopic Currents

The level of the holding potential also affected the relative amplitude of two components in the macroscopic current, although without significant effect on the kinetics of current inactivation (Fig. 5). The amplitudes of each component and their inactivation rate constants were obtained by fitting current traces to a sum of two exponentials (Eq. 6). When the test pulse was preceded by a 500-ms prepulse of different potentials (−160 vs −80 mV), the weight of the slow component was significantly altered, becoming smaller at the prepulse of −80 mV (Fig. 5 *C*). This indicates that the slow component of channel inactivation corresponds to I_H and that there are fewer channels in the slow mode at −80 mV (Fig. 5 *C*). However, there were no notable changes in the inactivation rate constants of either component (Fig. 5 *B*), indicating that gating kinetics was not altered in either mode by this maneuver. These results suggest that channels in the slow gating mode is more sensitive to a

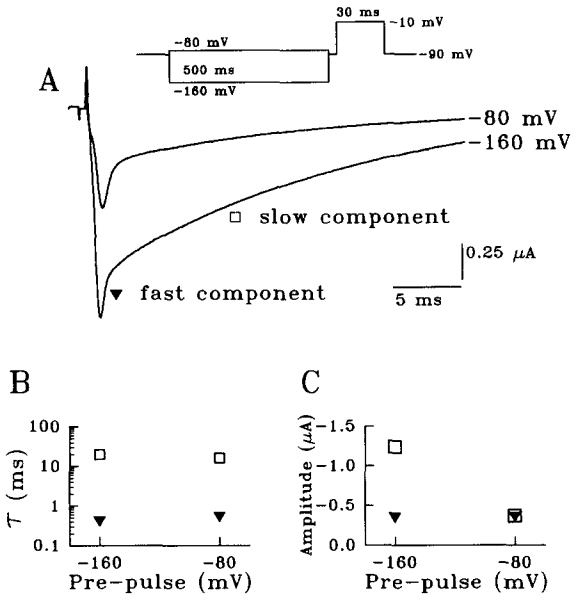

FIGURE 5. Effects of the prepulse on the relative amplitudes and inactivation kinetics of the fast and slow inactivating components in the macroscopic sodium current. (*A*) Current traces recorded at −10 mV preceded by a 500-ms prepulse of −80 or −160 mV. (*B*) Effects of the prepulse on current inactivation kinetics. Following a prepulse of −80 mV, τ_{fast} = 0.56 ms (▼) and τ_{slow} = 16.2 ms (□) and after a prepulse of −160 mV, τ_{fast} = 0.43 ms (▼) and τ_{slow} = 20.1 ms (□). (*C*) Effects of the prepulse on the relative amplitudes of the slow and fast components. At V_{pre} = −80 mV, I_{fast} = −0.36 μA and I_{slow} = −0.37 μA; at V_{pre} = −160 mV, I_{fast} = −0.37 μA and I_{slow} = −1.24 μA. Time constants and current amplitudes were obtained by fitting the current traces shown in Fig. 3 *A* to Eq. 6. Similar results were seen in three oocytes.

depolarizing change in membrane potential. Furthermore, the weight of the fast component was not significantly changed (−0.36 μA at V_{pre} = −80 mV vs −0.37 μA at V_{pre} −160 mV) while the weight of the slow component was greatly reduced, suggesting that there was no significant conversion of channels from one mode into the other during a 500-ms prepulse. Similar results were observed in three oocytes.

I-V Relationships and Current Activation

The effect of prepulse on the *I-V* relationship and current activation was also investigated. As expected, the inward peak current became significantly larger when the test pulses were preceded by a 500-ms prepulse of −180 mV (Fig. 6*A*). The

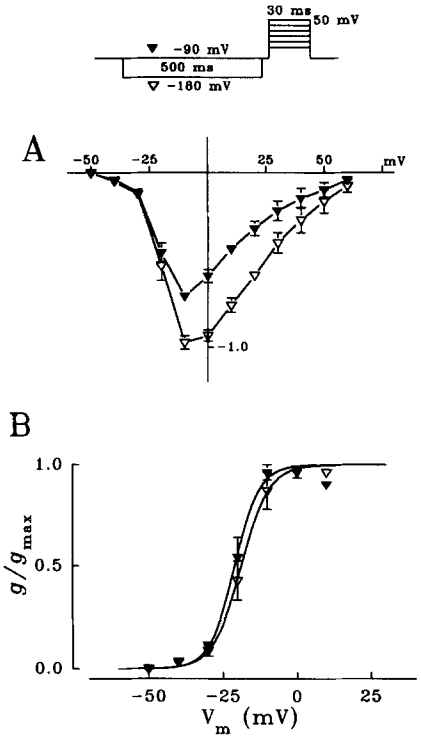

FIGURE 6. Effects of different prepulses on the activation of rat SkM1 sodium current. (*A*) Current-voltage relation curves recorded following a prepulse of −90 mV (▼) or −180 mV (▽) (n = 3). (*B*) Normalized current activation curves (n = 3). The procedure for normalization is described in the Materials and Methods. Solid curves are the best fits to Eq. 5. At V_{pre} = −90 mV (▼), $V_{1/2}$ = −20.9 mV, z = 4.8 e_0; at V_{pre} = −180 mV (▽), $V_{1/2}$ = −18.7 mV, z = 4.3 e_0.

maximal peak current was increased by 29.3 ± 2.3% (P < 0.01, paired t test, n = three oocytes). However, the shape of the *I-V* curves at different prepulses was very similar (Fig. 6*A*), suggesting that the voltage dependence of the current activation was not significantly changed. This is further shown by constructing current activation curves using normalized whole-cell sodium channel conductance (g_{Na} to $g_{Na,max}$, Eq. 5) (Fig. 6*B*, P > 0.05, paired t test, n = three oocytes). The voltage-dependent activation of the sodium channel, therefore, appears to be the same, independent of the inactivation gating mode it exhibits. This conclusion, however, is at variance with a previous report that the cumulative latency to first opening was different when single channels were in different kinetic modes at the same holding

potential (Zhou et al., 1991), and must be tempered by the fact that the two-electrode clamp may not accurately resolve the rising phase of the sodium channel activation. To clarify this discrepancy, further studies of the two modes will be needed at the single-channel level or with a macro-patch.

Effects of Coinjection of β_1 Subunit

Although modal gating of sodium channels has been observed in intact skeletal muscle fiber (Patlak and Ortiz, 1986), it is more prominent when rat SkM1 is

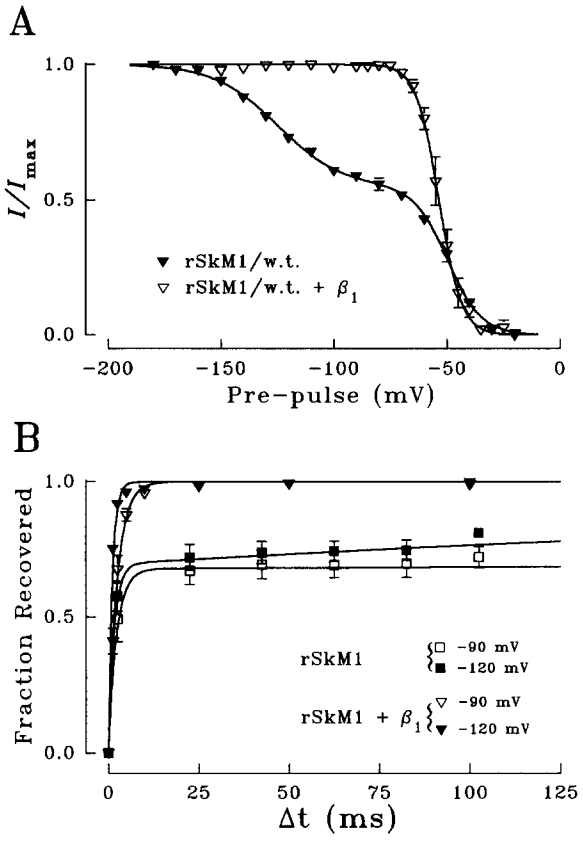

FIGURE 7. Effects of coinjection of α and β_1 subunits. (*A*) Effects on current inactivation. Solid curves are the best fits to Eqs. 1 and 2. For SkM1 alone (▼, $n = 5$), $V_{1/2,N} = -49.6$ mV, $Z_N = 3.2\ e_0$, and $W_N = 0.55$; $V_{1/2,H} = -124.7$ mV, $Z_H = 1.7\ e_0$, and $W_H = 0.45$. For SkM1 + β_1 subunit (▽, $n = 6$), $V_{1/2} = -53.4$ mV, $Z = 4.8\ e_0$. The voltage protocol was the same as shown in Fig. 1 *C*. (*B*) Effects on the recovery of current from inactivation. For rat SkM1 alone ($n = 3$), at $V_{hold} = -90$ mV (□), $\tau_{fast} = 2.3$ ms and $\tau_{slow} = 5.2$ s; at $V_{hold} = -120$ mV (■), $\tau_{fast} = 1.6$ ms and $\tau_{slow} = 376.6$ ms. After coinjection of α and β_1 subunits ($n = 6$), a single time constant was found. At $V_{hold} = -90$ mv (▽), $\tau = 2.3$ ms and at $V_{hold} = -120$ mV (▼), $\tau = 0.9$ ms. Solid lines are the best fits to Eqs. 3 and 4. The voltage protocol was the same as shown in Fig. 3 *B*.

expressed in *Xenopus* oocytes. rSkM1 expressed by transfection in mammalian cell lines, on the other hand, does not show this behavior (Ukomadu, Zhou, Sigworth, and Agnew, 1992). One possible explanation for the prevalence of H-mode gating in oocytes may be the absence of the β_1 subunit that is usually present in a 1:1 stoichiometry with the α-subunit in vivo (Barchi, 1988; Kraner, Tanaka, and Barchi, 1985; Roberts and Barchi, 1987). To test this possibility, we coinjected the oocytes with both α and β_1 cRNAs in a weight ratio of 1:1, corresponding to a molar ratio of 1:9, at which maximal restoration of the fast gating has been reported (Cannon,

McClatchey, and Gusella, 1993). The normalized inactivation curve of the resultant channels became monotonic and was well fit to a single exponential Boltzmann relation (Eq. 1, Fig. 7 *A*). Meanwhile, coexpression greatly accelerated the recovery of sodium current from inactivation and eliminated the slow-recovering component (Eq. 3, Fig. 7 *B*). As compared to the recovery without the β_1 subunit, at a holding potential of −90 mV, sodium current was fully recovered from inactivation within 10 ms instead of 30 s (Figs. 4 *B* and 7 *B*).

The effects of coinjection of α and β_1 subunits on the apparent current inactivation kinetics of the macroscopic current was also examined (Fig. 8). Unlike a previous report in which low molecular weight mRNA was coinjected with rSkM1 (Zhou et al., 1991), we found that the slow component was completely eliminated by coinjection in some oocytes (n = 2) (Fig. 8 *A*), whereas in others (n = 5), a slow inactivating component was still seen but with a much smaller weight (9% of the total current in

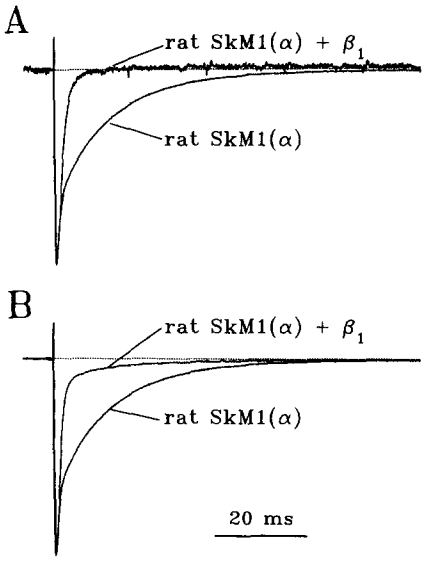

FIGURE 8. Effects of the coinjection of α and β_1 subunits on the kinetics of current inactivation. Sodium current was elicited by depolarizing the oocyte to −10 mV for 80 ms from a holding potential of −90 mV. In some oocytes, the slow inactivating component was completely eliminated after coinjection of α and β_1 subunits (*A*), whereas in others, a small amount of slowly inactivating current remained (for this recording, 9% of the total peak current after coinjection as compared with 64% beforehand) (*B*). In both *A* and *B*, the current traces have been normalized to each other.

the slow mode after coinjection as compared with 64% beforehand (Fig. 8 *B*). We reasoned that this could be due to either of two causes. First, there may not be enough β_1 subunits in the membrane to associate with α subunits after translation and posttranslational modification, in spite of the molar excess of β_1 cRNA. A second possibility is that the posttranslational modification of α subunit such as glycosylation may vary from oocyte to oocyte because it was reported that the cytoplasmic composition may deviate from one to another (Ruppersberg, Stocker, Pongs, Heinemann, Frank, and Koenen, 1991). To test the first possibility, we coinjected α and β_1 subunits in a weight ratio of 1:2, corresponding to a molar ratio of 1:18. Nonetheless, the slow component still appeared in some oocytes (data not shown). Therefore, the variability is more likely due either to the variations in the extent of posttranslational modification of α subunit in different oocytes, or to a manifestation of modal gating found in the intact skeletal muscle fiber.

DISCUSSION

Modal gating is a phenomenon that may be common to all voltage-dependent ion channels, including calcium (Hess, Lansman, and Tsien, 1984), potassium (McManus and Magleby, 1988), chloride (Blatz and Magleby, 1986) and sodium channels (see Introduction), and probably ligand-gated channels such as the acetylcholine receptor channel as well (Narajo and Brehm, 1993). It can be confirmed for a specific channel by satisfying the following criteria: (*a*) existence of multiple components with different kinetics in the same sample; (*b*) slow switching between different kinetic components in a single channel; and (*c*) a favored shift toward one component under a specific circumstance (Nilius, 1988). At the whole-cell level, there should be multiple kinetic components, and a particular component would be more favored under certain conditions, such as a change in membrane potential. In this report, we show that the sodium current recorded from oocytes injected with recombinant rSkM1 cRNA has two components (N- and H-components) and that each component has a different voltage dependence in its inactivation and its recovery from inactivation. The relative weight of the two components are modifiable under certain specific conditions: the N-component is favored by hyperpolarization and becomes more predominant when the β_1 subunit is coinjected with rSkM1.

One Channel with Two Gating Modes

The normalized inactivation curve for rSkM1 sodium channels expressed in oocytes has two components with different $V_{1/2}$'s, apparent gating valences, and relative weights (Fig. 1 and Table I). In addition to the previously described component that normally reaches its asymptote at membrane potentials more negative than −90 mV and has a $V_{1/2}$ of ~ −50 mV (referred to as normal current component, or I_N here), there is an additional component having a $V_{1/2}$ of ~ −130 mV, which we call the hyperpolarized current component (I_H). This biphasic relationship clearly differs from the h_∞ curves reported previously in nerve (Hodgkin and Huxley, 1952), muscle (Hille and Campbell, 1976), and in oocytes injected with sodium channel α subunit mRNA (Krafte et al., 1990).

One possible explanation for the phenomenon would be the presence of an intrinsic sodium current in oocytes (Baud, Kado, and Marcher, 1982), which differs in kinetics from the expressed rat SkM1 sodium current and therefore could contribute to the peculiar shape of the inactivation curve. If this were the case, a similar phemonenon should be seen when other sodium channel isoforms are expressed in oocytes. However, we never see a biphasic inactivation curve when the closely related rat SkM2 sodium channels are expressed in oocytes and examined using a comparable voltage protocol (Fig. 1, *B* and *C*). Additionally, this hypothesis is not supported by the effects of varying membrane potential (Fig. 2) and the effects of coinjection of α and β_1 subunits (Fig. 7). Furthermore, there was no intrinsic sodium current observed in our control oocytes.

A second possibility is that variant forms of SkM1 were synthesized in the oocytes due to improper translation or posttranslational modification of the recombinant cRNA injected. If this were true, we would expect considerable variability in the relative weight of two components for a given voltage condition, yet little variation

was seen (Fig. 1 *C*). This possibility is also inconsistent with the ability of membrane potential to cause an interconversion between the two modes of inactivation (Fig. 2 *A*).

A more likely explanation is that the expressed SkM1 sodium channels in oocytes can enter either of two gating modes that differ in their voltage-dependent kinetics of inactivation and recovery from inactivation. This is consistent with the observed regulation in the relative weights of the two components by voltage. As shown in Fig. 2 *A*, the weight of the I_H decreases as the holding potential becomes more negative and finally disappears at a holding potential of −140 mV, indicating a voltage-dependent interconversion of channels from one mode into the other. The weights and rates of the two components found during the time course of current recovery from inactivation are also highly voltage dependent (Fig. 4 *B*), with the slow-recovering component more sensitive to a change of the holding potential from −90 to −120 mV. Similarly, the relative weights of the fast and slow inactivating components are altered as the voltage of a 500-ms prepulse is changed (−80 vs −160 mV), with the weight of the slow one much more affected than that of the fast one (Fig. 5). Clearly, these data support the notion that the expressed SkM1 sodium channel can exist in either a normal (N-mode) or an abnormal (H-mode) mode, and that the two modes are regulated differently by voltage, but interconvertible.

Voltage-dependent Mode Interconversion

Our first-order two-state reaction model analysis indicates that the modal interconversion has it characteristic voltage dependence, which may arise from the fact that both forward and backward rate constants have an exponential dependence on membrane potential, with the backward rate (β) being approximately three times as voltage dependent as the forward rate (α) (Fig. 3 *C*). Voltage dependence is also found for the interconversion of kinetic modes in the voltage-gated L-type cardiac Ca^{2+} channel (Pietrobon and Hess, 1990). However, in contrast to this Ca^{2+} channel, the equilibrium between N- and H-modes in rSkM1 sodium channel is not as steeply voltage dependent as normal channel activation and inactivation. This raises the question of the molecular identity of the voltage sensor for modal interconversion and its relationship to the voltage gate of sodium channel activation. One possibility is that the S4 segment, usually considered to be the voltage sensor for the activation of voltage-gated ion channels (Guy, 1988), is also the voltage sensor for the mode interconversion. However, modal interconversion is approximately four orders of magnitude slower than activation. Therefore, a very slow intermediate process must be coupled to the voltage-dependent movement of one or more of the S4 segments to prompt the interconversion. Another possibility is that the modal interconversion has its own, yet to be identified, voltage sensor. However, this voltage sensor cannot be determined from presently available data. Its molecular identify awaits site-directed mutagenic experiments in combination with careful kinetic analysis.

Effects of the β_1 Subunit

The adult rat skeletal muscle sodium channel (rSkM1) is a hetero-oligomeric protein, consisting of one large α-subunit (260–280 kD) and one small β_1 subunit (~36 kD)

(Barchi, 1988; Kraner et al., 1985; Roberts and Barchi, 1987). When expressed alone in oocytes, the α-subunit can form a functional channel, although it exhibits an abnormal predominance of slow gating in its inactivation and recovery from inactivation (Auld et al., 1988; Krafte et al., 1990; Moorman et al., 1990; Zhou et al., 1991). Recent evidence shows that a β_1 subunit, found originally in brain (Isom, De Jongh, Patton, Reber, Offord, Charbonneau, Walsh, Goldin, and Catterall, 1992) and also expressed in skeletal and cardiac muscle (Yang, Bennett, Makita, George, and Barchi, 1993), is selectively associated with the SkM1 α-subunit during development and after denervation in rat muscle, suggesting a possible functional association between these two subunits (Yang *et al.*, 1993). Normal fast inactivation is restored when SkM1 is expressed with this rat β_1 subunit (Bennett et al., 1993; Yang et al., 1993), and we show here that coinjection of this β_1 subunit abolishes I_H in the inactivation curve (Fig. 7). One interpretation of these findings is that the binding of β_1 to α stabilizes a conformation of the α subunit that favors the normal gating mode.

The fast inactivation of the sodium channel has been modeled in a ball-and-chain formulation (Armstrong and Bezanilla, 1977; Bezanilla and Armstrong, 1977): the channel inactivates as a tethered "ball" binds to its inner mouth after the outward propagation of the activation gate in response to a membrane potential change (Guy, 1988). The molecular counterpart for this ball has been suggested to be the cytoplasmic loop between domains 3 and 4 (Stühmer, Conti, Suzuki, Wang, Noda, Yahagi, Kubo, and Numa, 1989; West, Patton, Scheuer, Wang, Goldin, and Catterall, 1992) while its receptor is probably formed by other elements on the cytoplasmic surface of the α subunit. The α subunit may exist in two interconvertible conformations, one of which favors the binding of this cytoplasmic loop more strongly than the other, as evidenced by fast versus slow gating. In the absence of the β_1 subunit, the distribution of channel molecules between these two conformations is in a steady state with the conformation exhibiting slow gating mode more favored. At hyperpolarized holding potentials the conformation showing fast inactivation is preferred (Fig. 2 *A*). Coinjection of the β_1 subunit may also stabilize the channel in this conformation, shifting the steady state distribution of the channels between two conformations (*I*) Fig. 8). However, the inactivation properties of the N-component are not identical to those observed in the presence of β_1. Besides that, the $V_{1/2}$ shifted in the hyperpolarized direction by ~ -4 mV (Fig. 7 *A*), the N-component in the absence of β_1 has less voltage dependence than in its presence (3.3 vs 4.8 elementary charges). Because steady state inactivation derives much of its voltage dependence from coupling with activation (Armstrong and Bezanilla, 1977; Bezanilla and Armstrong, 1977), our data suggest that the presence of β_1 facilitates this coupling.

If, as our data suggest, there are two gating modes available to the sodium channel, can we identify a biphasic inactivation curve for sodium channels in skeletal muscle fibers under physiological conditions? Although theoretically possible, the low probability of the H-mode in vivo would make this very difficult. It has been estimated that current through the long-bursting channels, kinetically, which correspond to the H-mode channels, may account for only 0.12% of the peak sodium current in skeletal muscle (Patlak and Ortiz, 1986). The contribution of this small component of the current to the overall shape of the h_∞ curve would be extremely difficult to detect.

Conclusions

Our results demonstrate that the rat SkM1 sodium current expressed in oocytes has two components attributable to channels which inactivate and recover from inactivation differently in terms of their voltage and time dependence, and that channels can interconvert between these modes as a voltage-dependent process. The prominence of the two modes may be a consequence of alternate tertiary structures assumed by rat SkM1 when expressed in oocytes in the absence of a β_1 subunit, implicating the binding of β_1 as a factor in stabilizing the physiologically preferred channel conformation.

This work was in part supported by NIH grants NS-18013 (R. L. Barchi) and AR-41691 (R. Horn) and a grant from the Muscular Dystrophy Association (R. L. Barchi). S. Ji is a recipient of the Muscular Dystrophy Association Research Fellowship. A. L. George is a Lucille P. Markey Scholar.

Original version received 13 October 1993 and accepted version received 10 May 1994.

REFERENCES

Aldrich, R. W., D. P. Corey, and C. F. Stevens. 1983. A reinterpretation of mammalian sodium channel gating based on single channel recording. *Nature.* 306:436–441.

Armstrong, C. M., and F. Bezanilla. 1977. Inactivation of the sodium channel. II. Gating current experiments. *Journal of General Physiology.* 70:567–590.

Auld, V. J., A. L. Goldin, D. S. Krafte, J. Marshall, J. M. Dunn, W. A. Catterall, H. A. Lester, N. Davidson, and R. J. Dunn. 1988. A rat brain Na^+ channel α subunit with novel gating properties. *Neuron.* 1:449–461.

Barchi, R. L. 1988. Probing the molecular structure of the voltage-dependent sodium channel. *Annual Review of Neuroscience.* 11:455–495.

Baud, C., R. T. Kado, and K. Marcher. 1982. Sodium channels induced by depolarization of the *Xenopus laevis* oocyte. *Proceedings of National Academy of Sciences, USA.* 79:3188–3192.

Bennett, P. B., N. Makita, and A. L. George. 1993. A molecular basis for gating mode transitions in human skeletal muscle Na^+ channels. *FEBS Letters.* 326:21–24.

Bezanilla, F., and C. M. Armstrong. 1977. Inactivation of the sodium channel. I. Sodium current experiments. *Journal of General Physiology.* 70:549–566.

Blatz, A. L., and K. L. Magleby. 1986. Quantitative description of three modes of activity of fast chloride channels from rat skeletal muscle. *Journal of Physiology.* 378:141–174.

Cannon, S. C., A. I. McClatchey, and J. F. Gusella. 1993. Modification of the Na^+ current conducted by the rat skeletal muscle α subunit by coexpression with a human brain β subunit. *Pflügers Archiv.* 423:155–157.

Chahine, M., L.-Q. Chen, R. L. Barchi, R. G. Kallen, and R. Horn. 1992. Lidocaine block of human heart sodium channels expressed in *Xenopus* oocytes. *Journal of Molecular and Cellular Cardiology.* 24:1231–1236.

Goldin, A. L. 1992. Maintenance of *Xenopus laevis* and oocyte injection. *Methods in Enzymology.* 207:266–279.

Guy, H. R. 1988. A model relating structure of the sodium channel to its function. *Current Topics in Membrane Transport.* 33:289–308.

Hess, P., J. B. Lansman, and R. W. Tsien. 1984. Different modes of Ca channel gating behavior favored by dihydropyridine Ca agonists and antagonists. *Nature.* 311:538–544.

Hille, B., and D. T. Campbell. 1976. An improved vaseline gap voltage clamp for skeletal muscle fibers. *Journal of General Physiology.* 67:265–293.

Hodgkin, A. L., and A. F. Huxley. 1952. Currents carried by sodium and potassium ions through the membrane of the giant axon of *Loligo*. *Journal of Physiology*. 116:449–472.

Horn, R., and C. A. Vandenberg. 1984. Statistical properties of single sodium channels. *Journal of General Physiology*. 84:505–534.

Howe, J. R., and J. M. Ritchie. 1992. Multiple kinetic components of sodium channel inactivation in rabbit Schwann cells. *Journal of Physiology*. 455:529–566.

Isom, L. L., K. S. De Jongh, D. E. Patton, B. F. X. Reber, J. Offord, H. Charbonneau, K. Walsh, A. L. Goldin, and W. A. Catterall. 1992. Primary structure and functional expression of the β_1 subunit of the rat brain sodium channel. *Science*. 256:839–842.

Kallen, R. G., Z.-H. Sheng, J. Yang, L. Chen, R. B. Rogart, and R. L. Barchi. 1990. Primary stricture and expression of a sodium channel characteristic of denervated and immature rat skeletal muscle. *Neuron*. 4:233–242.

Kirsch, G. E., and A. M. Brown. 1989. Kinetic properties of single sodium channels in rat heart and rat brain. *Journal of General Physiology*. 93:85–99.

Kiyosue, T., and M. Arita. 1988. Late sodium current and its contribution to action potential configuration in guinea pig ventricular myocytes. *Circulation Research*. 64:389–397.

Krafte, D. S., A. L. Goldin, V. J. Auld, R. J. Dunn, N. Davidson, and H. A. Lester. 1990. Inactivation of cloned Na channels expressed in *Xenopus* oocytes. *Journal of General Physiology*. 96:689–706.

Krafte, D. S., and H. A. Lester. 1992. Use of stage II-III *Xenopus* oocytes to study voltage-dependent ion channels. *Methods in Enzymology*. 207:339–345.

Kraner, S. D., J. C. Tanaka, and R. L. Barchi. 1985. Purification and functional reconstitution of the voltage-sensitive sodium channel from rabbit T-tubular membranes. *Journal of Biological Chemistry*. 260:6341–6347.

McManus, O. B., and K. L. Magleby. 1988. Kinetic states and modes of single large-conductance calcium-activated potassium channels in cultured rat skeletal muscle. *Journal of Physiology*. 402:79–120.

Moorman, J. R., G. E. Kirsch, A. M. J. VanDongen, R. H. Joho, and A. M. Brown. 1990. Fast and slow gating of sodium channels encoded by a single mRNA. *Neuron*. 4:243–252.

Naranjo, D., and P. Brehm. 1993. Modal shifts in acetylcholine receptor channel gating confer subunit-dependent desensitization. *Science*. 260:1811–1814.

Nilius, B. 1988. Modal gating behavior of cardiac sodium channels in cell-free membrane patches. *Biophysical Journal*. 53:857–862.

Patlak, J. 1991. Molecular kinetics of voltage-dependent Na^+ channels. *Physiological Reviews*. 71:1047–1080.

Patlak, J. B., and M. Ortiz. 1985. Slow currents through single sodium channels of the adult rat heart. *Journal of General Physiology*. 86:89–104.

Patlak, J. B., and M. Ortiz. 1986. Two modes of gating during late Na^+ channel currents in frog sartorius muscle. *Journal of General Physiology*. 87:305–326.

Pietrobon, D., and P. Hess. 1990. Novel mechanism of voltage-dependent gating in L-type calcium channels. *Nature*. 346:651–655.

Quandt, F. N. 1987. Burst kinetics of sodium channels which lack fast inactivation in mouse neuroblastoma cells. *Journal of Physiology*. 392:563–585.

Roberts, R. H., and R. L. Barchi. 1987. The voltage-sensitive sodium channel from rabbit skeletal muscle: chemical characterization of subunits. *Journal of Biological Chemistry*. 262:2298–2303.

Ruppersberg, J. P., M. Stocker, O. Pongs, S. H. Heinemann, R. Frank, and M. Koenen. 1991. Regulation of fast inactivation of cloned mammalian I_k (A) channels by cysteine oxidation. *Nature*. 352:711–714.

Sigworth, F. J., and E. Neher. 1980. Single Na^+ channel currents observed in cultured rat muscle cells. *Nature.* 287:447–449.

Stühmer, W. 1992. Electrophysiological recording from *Xenopus* oocytes. *Methods in Enzymology.* 207:319–339.

Stühmer, W., F. Conti, H. Suzuki, X. Wang, M. Noda, N. Yahagi, H. Kubo, and S. Numa. 1989. Structural parts involved in activation and inactivation of the sodium channel. *Nature.* 339:597–603.

Trimmer, J. S., S. S. Cooperman, S. A. Tomiko, J. Zhou, S. M. Crean, M. B. Boyle, R. G. Kallen, Z. Sheng, R. L. Barchi, F. J. Sigworth, R. H. Goodman, W. S. Agnew, and G. Mandel. 1989. Primary structure and functional expression of a mammalian skeletal muscle sodium channel. *Neuron.* 3:33–49.

Ukomadu, C., J. Zhou, F. J. Sigworth, and W. S. Agnew. 1992. μI Na^+ channels expressed transiently in human embryonic kidney cells: biochemical and biophysical properties. *Neuron.* 8:663–676.

West, J. W., D. E. Patton, T. Scheuer, Y. Wang, A. L. Goldon, and W. A. Catterall. 1992. A cluster of hydrophobic amino acid residues required for fast Na^+-channel inactivation. *Proceedings of National Academy of Sciences, USA.* 89:10910–10914.

Yang, J. S., P. B. Bennett, N. Makita, A. L. George, and R. L. Barchi. 1993. Expression of the sodium channel β_1 subunit in rat skeletal muscle is selectively associated with the tetrodotoxin-sensitive α subunit isoform. *Neuron.* 11:915–922.

Zhou, J., J. F. Potts, J. S. Trimmer, W. S. Agnew, and F. J. Sigworth. 1991. Multiple gating modes and the effect of modulating factors on the μI sodium channel. *Neuron.* 7:775–785.